Appl Phys A (2012) 107:971–975
DOI 10.1007/s00339-012-6850-5

Applied Physics A
Materials Science & Processing

Low-threshold ZnO random lasing in a homojunction diode with embedded double heterostructure

Jieying Kong · Sheng Chu · Zheng Zuo · Jingjian Ren · Mario Olmedo · Jianlin Liu

Received: 25 July 2011 / Accepted: 17 February 2012 / Published online: 17 March 2012

Abstract An electrically pumped random laser diode was fabricated with a MgZnO/ZnO/MgZnO double heterostructure embedded in a ZnO pn junction. Gain can be achieved at very low-threshold current owing to exciton processes. Light closed loops are formed by random multiple scattering on vertical column boundaries in the thin film. The tilted and rough mesa edge planes serve as refraction mirrors, giving rise to surface emission.

1 Introduction

Small, versatile semiconductor laser diodes (LD) play an important role in daily life in the fields of healthcare, information storage, and defense. Lowering the threshold current is a key goal on which scientists and engineers made a great deal of efforts in the past half century, since the first LD based on GaAs p-n junction structure was reported [1]. A breakthrough in electrically pumped devices came from the idea of double heterojunction structure, which realizes coincidence and concentration of recombination, light emission and population inversion in the same gain layer, hence the dramatic decrease of threshold current. However, it is still too high for many applications [2, 3]. For wide bandgap semiconductor materials, a high carrier concentration is usually required in order to reach an optical gain that is high enough for lasing action in an electron-hole plasma (EHP) process [4]. The EHP mechanism, which is common for conventional LD operation, typically requires high threshold current density. Exciton lasing, as an alternative, is a more efficient radiative process and can facilitate low-threshold stimulated emission owing to its bosonic nature [5]. However, in some semiconductor materials such as III-V nitride and GaAs, the exciton binding energies are too small to sustain thermal interruption, so excitonic emission was only observed in the low-dimensional structures [6, 7]. In contrast, ZnO has a native exciton binding energy of 60 meV, which enables excitonic gain even without low-dimensional quantum confinement [8].

Although ZnO has potential as an alternative to III-V nitride, it is still underdeveloped due to the difficulty of p-type doping [9], which hinders the realization of electrically pumped LDs. Compared to electrically pumped cleaved-crystal GaN diode laser, most ZnO lasers are unconventional, including optically pumped disordered particles [10], optically pumped nanowires [11], and electrically pumped metal-oxide-semiconductor laser [12]. Electrically pumped pn-junction laser diodes using ZnO-based heterostructures have been rarely reported [13, 14]. Due to diffusion of Mg and Be, the heterostructures with very thin quantum wells embedded in the p-n junctions virtually become MgZnO, and BeZnO barrier layers, respectively [15, 16]. Therefore, the mechanism of lasing in these device structures remains unclear. In this paper, we report a diode with embedded MgZnO/ZnO/MgZnO double heterostructure (DH), where the MgZnO barrier is relatively thick and the ZnO well is wide. This device clearly differs from existing devices [13, 14] in terms of existence of a true ZnO quantum well in the p-n junction. The device exhibits random lasing at room temperature, owing to carrier-exciton interaction in the MgZnO/ZnO/MgZnO heterostructure and light multiple scattering. The results show that low-threshold current is feasible even if the hole carrier concentration is not sufficiently high enough to form EHP.

J. Kong · S. Chu · Z. Zuo · J. Ren · M. Olmedo · J. Liu (✉)
Quantum Structures Laboratory, Department of Electrical Engineering, University of California at Riverside, Riverside, CA 92521, USA
e-mail: jianlin@ee.ucr.edu

2 Experimental results and discussion

Figure 1 shows a schematic of the ZnO-based DH device. The structure was grown on n-type Si (100) substrate (1–20 Ω·cm) using plasma-assisted molecular beam epitaxy (MBE). A thin magnesium oxide (MgO) buffer layer was first deposited at 350 °C to reduce the lattice mismatch between Si and ZnO, followed by 200 nm Ga-doped n-ZnO at 550 °C. After the growth of n-ZnO, a $Mg_{0.1}Zn_{0.9}O$/intrinsic ZnO/$Mg_{0.1}Zn_{0.9}O$ heterostructure was grown. Subsequently, the temperature was increased to 600 °C and 200 nm Sb-doped p-ZnO was grown. High-temperature post-annealing at 750 °C was performed to activate acceptor dopants.

As-grown sample exhibits loosely packed columnar structures with in-plane size of 200 nm on average as a result of large lattice mismatch between Si and ZnO, which are clearly seen in the scanning electron microscope (SEM) image in the inset of Fig. 2(a). Figure 2(a) shows x-ray diffraction (XRD) $\theta/2\theta$ scan spectrum of the diode, indicating that the film grows preferentially along the c-direction of the ZnO wurtzite lattice. The sample was etched down to Ga-doped ZnO layer via standard photolithography process and mesa of 800 μm × 800 μm was defined. Au/Ti and Au/NiO were deposited on the bottom Ga-doped layer and top Sb-doped layer, respectively, after which the proper temperature annealing was carried out to form good Ohmic contacts.

The elemental distribution of Zn, O, Mg, Ga, Sb and Si was obtained by performing secondary ion mass spectroscopy (SIMS) measurements, and the result is shown in Fig. 2(b). Clear MgZnO/ZnO/MgZnO structure is inferred at around 200 nm depth under surface. The ZnO well width was determined to be 30 nm. Also, the Sb signal extends from the top ZnO layer into the upper MgZnO layer, which may give rise to a more efficient hole supply reservoir. A strong Mg signal near the interface of ZnO and Si substrate indicates the existence of MgO/ZnO buffer layer.

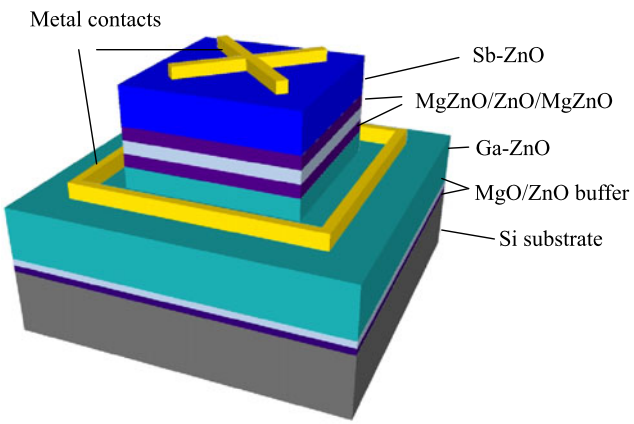

Fig. 1 Schematic of the LD device

Figure 3 shows the current-voltage characteristics of the laser device. The insets show ohmic behaviors of n-contacts and p-contacts. The rectifying characteristic between n- and p-contacts suggests that a p-n diode should be formed. The turn-on voltage can be determined to be about 5 V. Lasing emission was collected from mesa surface as the diode was biased under DC forward voltages. Figure 4 shows the electroluminescence (EL) spectra of the diode. Clear lasing occurs as drive current increases above 30 mA. Both the number and intensity of sharp lasing mode peaks in the spectral region increase as the injection current increases. Some lasing modes also disappear at the higher injection currents. The lasing modes are determined by the path of the closed-loop random cavities. Since the closed loops are randomly formed by scattering, it is possible that under different injection currents, the paths of closed loops are different. Overall, there is higher possibility of the formation of additional random cavities at higher currents. It is a typical phenomenon for a random laser, and is widely observed in electrically pumped and optically pumped ZnO-based devices [10–12]. The top inset shows the typical full wavelength EL spectrum from the device, which covers from 350 nm to 650 nm.

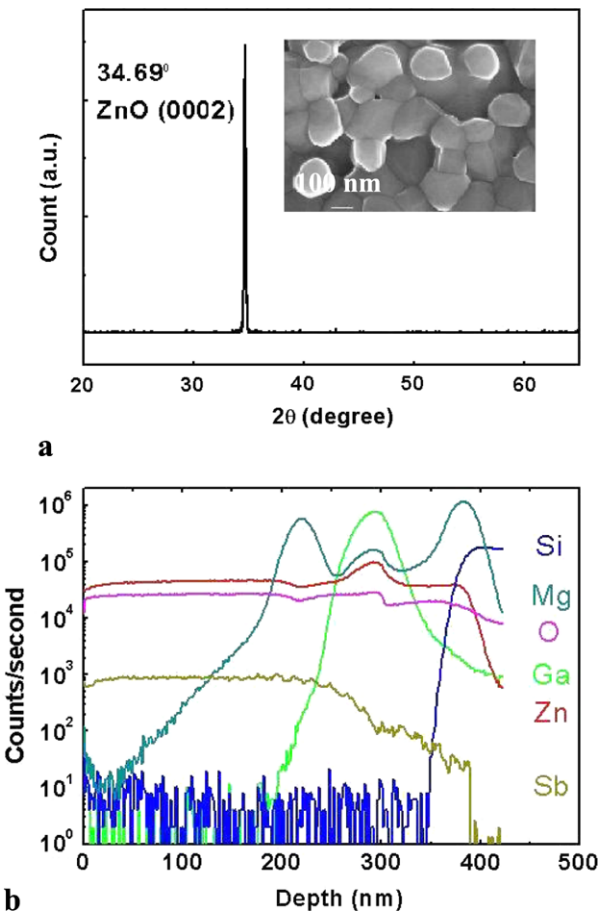

Fig. 2 (**a**) XRD $\theta/2\theta$ result showing preferential (0001) growth. *Inset* is top-view SEM image of as-grown sample. (**b**) SIMS spectra of the sample, showing elemental distribution of Zn, O, Mg, Ga and Sb

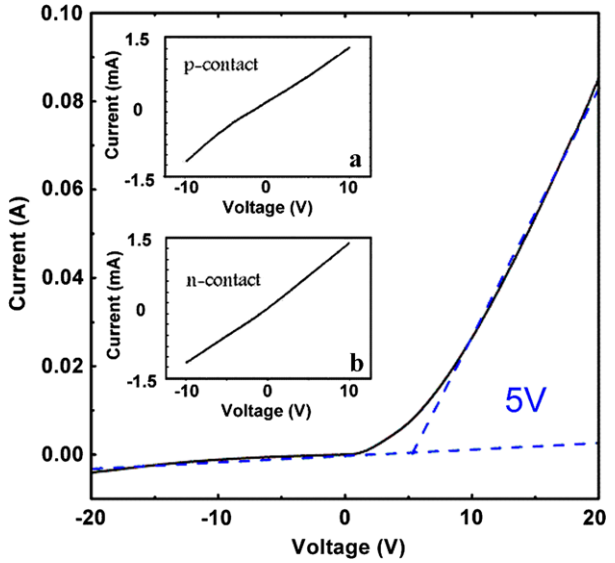

Fig. 3 Current-voltage characteristic of a typical diode. *Insets* show that Ohmic contacts were formed for p-type ZnO layer and n-type ZnO layer, respectively

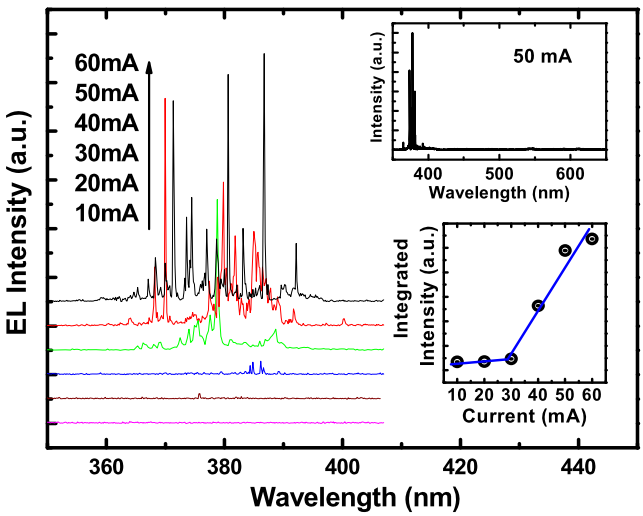

Fig. 4 Room temperature EL spectra at the injection current from 10 mA to 60 mA. The *top inset* is a typical full wavelength recording, showing no deep level emission, and the *bottom inset* is integrated intensity vs. injection current

Near band edge emission is dominant compared to weak deep level emissions. Furthermore, there is no indication of EHP formation since the center of lasing peaks is almost at the same position of 380 nm when the injection current increases from 10 mA to 60 mA, as shown in Fig. 4. In normal EHP case, EHP recombination comes at the lower energy tail of excitonic emission, and has an evident red-shift as pumping power increases [17, 18], which is mainly due to band-gap renormalization with excess carrier density larger than Mott density.

The plot of the integrated lasing spectrum intensity as a function of injection current is shown in the lower inset of Fig. 4. A solid line is plotted to guide the eyes, showing the threshold current of about 30 mA, corresponding to current density of 4.7 A/cm^2. The threshold current density is given approximately by $J_{\rm th} = eN_{\rm th}d/\tau$, where e is the electron charge, $N_{\rm th}$ is the carrier density at the threshold, d is the active layer thickness. Assuming the exciton lifetime to be 100 ps [19], and the active layer thickness to be 30 nm according to the SIMS profile, $N_{\rm th}$ is calculated to be 3×10^{15} cm^{-3}. This number is much smaller than the Mott density of 5×10^{17} cm^{-3} in ZnO [20], suggesting that the gain in this diode laser should originate from an excitonic process rather than EHP process. Low hole carrier concentrations may be enough for excitonic lasers in a theoretical prediction [8]. For Sb doping, a higher hole concentration of up to 10^{18} cm^{-3} was achieved [21]; therefore, it confirms that p-type doping of ZnO, although difficult, may create sufficient hole carrier concentrations for realizing low-threshold electrically pumped random lasers. It should be noted that this estimation does not consider the current crowding effect where mesa edge and center areas carry larger current density than other areas on the mesa due to the current spreading from bottom electrode and top electrode, respectively. Nevertheless, we argue that the current density near the mesa edge areas is still not large enough to generate an EHP process as the lasing spectrum does not red-shift at higher injection currents.

A dynamic view of excitonic recombination is plotted in Fig. 5(a). At the forward bias condition, electrons and holes are injected from Ga-doped ZnO layer and Sb-doped ZnO layer, respectively, and trapped into the central ZnO well layer within MgZnO barriers. Recombination occurs mainly in the central ZnO layer, where electrons and holes form excitons through the electron-hole Coulomb interaction. Further injection of electrons and holes into the ZnO well at higher biases leads to carrier-exciton interaction with photon emissions and gain.

In addition to the creation of optical gain, light multiple scattering to form closed loops to amplify stimulated emission is required in random lasing. In this device, as schematically shown in Fig. 5(b), the closed loops could be formed by random scattering via vertical column boundaries in the thin film, with pores or air gaps in between each other, acting as multi-faceted scattering media; or back-and-forth reflections at the parallel side walls. These air gaps play important roles in enhancing the light scattering due to its refractive index difference with ZnO; without these air gaps, the diodes with similar MgZnO/ZnO/MgZnO heterostructures showed no lasing or weak lasing on Si and sapphire substrates, respectively [15, 22]. Since the column boundary planes are vertical to the substrate, the closed loops of the light are formed in the film plane rather than in the

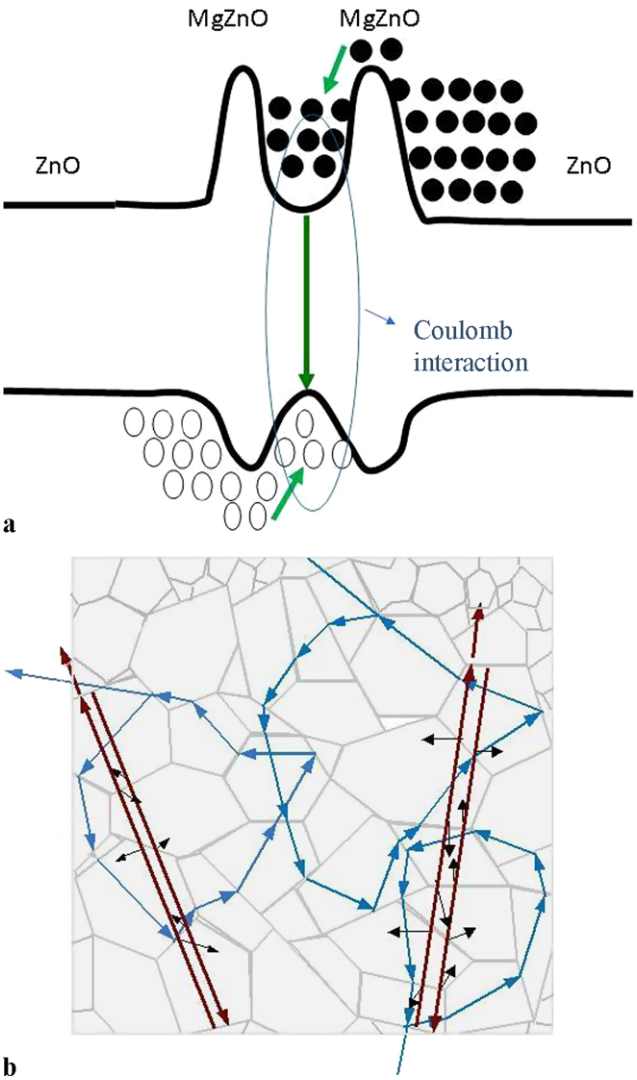

Fig. 5 (**a**) Band diagram and dynamic view of exciton formation and electron-exciton interaction process. (**b**) Schematic view of random laser closed loops from light multiple scattering, including random scattering from multiple planes and two parallel planes

growth direction, leading to edge emission, rather than surface emission [23, 24]. An image of a working device at drive current of 30 mA was taken by microscope camera in dark background, as shown in Fig. 6(a). The edge emission is dominant compared to surface emission, indicating that the closed loops are indeed formed in the film plane. Note that a conventional edge emitting LD normally requires the polishing of the edge or perfect cleave of the crystal [25], however, in ZnO case, the perfect cleavage along parallel crystal planes is difficult as its hexagonal crystal structures would not be as easily cleaved with flat planes as those cubic crystals. In the present LD, no polishing process was done on the edge except a standard mesa wet chemical etching in the device fabrication process. Therefore, side planes of the diode mesa are not completely perpendicular to the substrates, as shown in the SEM image in Fig. 6(b). Figure 6(c)

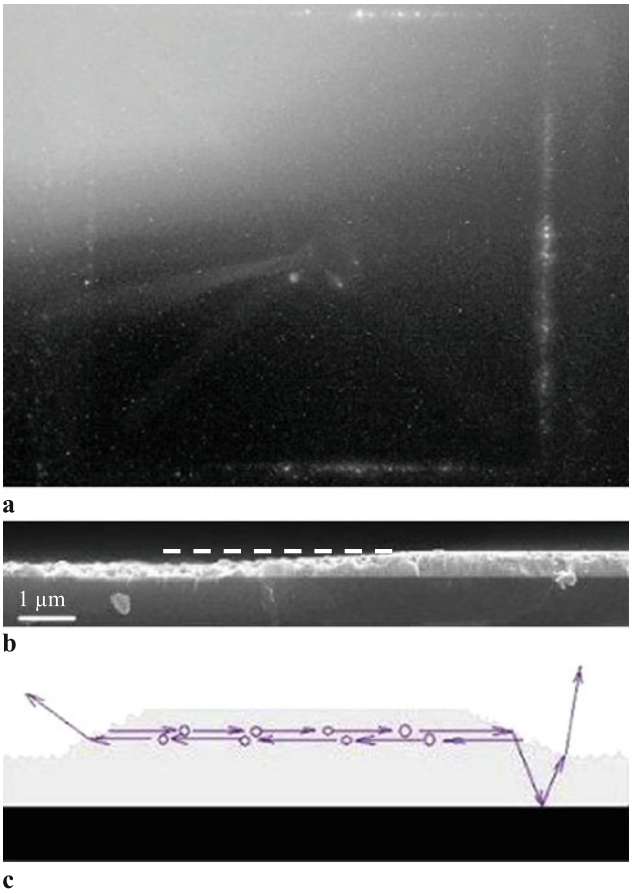

Fig. 6 (**a**) Image of a working device taken by microscope camera at dark background with drive current 30 mA. (**b**) SEM side view of mesa edge of the diode. The *dashed line*, which is on the same plane of the mesa surface, is drawn to guide the eyes to see the tilted and rough mesa edge plane. (**c**) Schematic explanation of the output paths of scattered lights. Only one closed loop is drawn for clarity

draws possible paths for scattered light from a closed loop to escape from the device. It is evident that once the lasing light, refracted light from an in-plane closed-loop random cavity, is incident onto the tilted and rough edge plane of the mesa, it will be reflected/refracted by this plane to emit into all directions.

3 Conclusion

We experimentally realized an electrically pumped random laser with a MgZnO/ZnO/MgZnO heterostructure embedded in a ZnO p-n junction at room temperature. Due to excitonic process, the threshold current is low. Moreover, naturally grown columns provide multiple scattering media at boundaries, giving rise to the formation of random closed loops, hence the laser has randomly distributed peaks. The observation of random laser in this device confirms that the recent achievement of p-type doping is sufficient for realization of low-threshold electrically pumped laser.

Acknowledgements This work is supported by the Army Research Office (ARO) under the Young Investigator Program (YIP) grant of W911NF-08-1-0432 and the National Science Foundation (ECCS-0900978).

References

1. R.N. Hall, G.E. Fenner, J.D. Kingsley, T.J. Soltys, R.O. Carlson, Phys. Rev. Lett. **9**, 366 (1962)
2. Zh.I. Alferov, R.F. Kazarinov, No. Inventor's Certificate, 181737 (in Russian)
3. H. Kroemer, Proc. IEEE **51**, 1782 (1963)
4. C. Klingshirn, J. Cryst. Growth **117**, 753 (1992)
5. A. Imamoglu, R.J. Ram, S. Pau, Y. Yamamoto, Phys. Rev. A **53**, 4250 (1996)
6. W. Wegscheider, L.N. Pfeiffer, M.M. Dignam, A. Pinczuk, K.W. West, S.L. McCall, R. Hull, Phys. Rev. Lett. **71**, 4071 (1993)
7. S.F. Chichibu, T. Azuhata, T. Sota, T. Mukai, Appl. Phys. Lett. **79**, 341 (2001)
8. M. Zamfirescu, A. Kavokin, B. Gil, G. Malpuech, M. Kaliteevski, Phys. Rev. B **65**, 161205(R) (2002)
9. C.G. Van de Walle, Phys. Rev. Lett. **85**, 1012 (2000)
10. H. Cao, Y.G. Zhao, H.C. Ong, S.T. Ho, J.Y. Dai, J.Y. Wu, R.P.H. Chang, Appl. Phys. Lett. **73**, 3656 (1998)
11. M.H. Huang, S. Mao, H. Feick, H. Yan, Y. Wu, H. Kind, E. Weber, R. Russo, P. Yang, Science **292**, 1897 (2001)
12. X. Ma, P. Chen, D. Li, Y. Zhang, D. Yang, Appl. Phys. Lett. **91**, 251109 (2007)
13. S. Chu, M. Olmedo, Z. Yang, J. Kong, J. Liu, Appl. Phys. Lett. **93**, 181106 (2008)
14. Y.R. Ryu, J.A. Lubguban, T.S. Lee, H.W. White, T.S. Jeong, C.J. Youn, B.J. Kim, Appl. Phys. Lett. **90**, 131115 (2007)
15. S. Chu, J. Zhao, Z. Zuo, J. Kong, L. Li, J. Liu, (2012) (unpublished)
16. C. Klingshirn, J. Fallert, Z. Huijuan, H. Kalt, Appl. Phys. Lett. **91**, 126101 (2007)
17. J. Dai, C.X. Xu, P. Wu, J.Y. Guo, Z.H. Li, Z.L. Shi, Appl. Phys. Lett. **97**, 011101 (2010)
18. M. Kawasaki, A. Ohtomo, I. Ohkubo, H. Koinuma, Z.K. Tang, P. Yu, G.K. L Wang, B.P. Zhang, Y. Segawa, Mater. Sci. Eng. B, Solid-State Mater. Adv. Technol. **56**, 239 (1998)
19. T. Koida, S.F. Chichibu, A. Uedono, A. Tsukazaki, M. Kawasaki, T. Sota, Y. Segawa, H. Koinuma, Appl. Phys. Lett. **82**, 532 (2003)
20. C. Klinshirn, R. Hauschild, J. Fallert, H. Kalt, Phys. Rev. B **75**, 115203 (2007)
21. F.X. Xiu, Z. Yang, L.J. Mandalapu, D.T. Zhao, J.L. Liu, W.P. Beyermann, Appl. Phys. Lett. **87**, 152101 (2005)
22. J. Kong, L. Li, Z. Yang, J. Liu, J. Vac. Sci. Technol. B **28**(3), C3D10 (2010)
23. S. Gottardo, S. Cavalieri, O. Yaroshcuk, D.S. Wiersma, Phys. Rev. Lett. **93**, 263901 (2004)
24. S.P. Lau, H.Y. Yang, S.F. Yu, H.D. Li, M. Tanemura, T. Okita, H. Hatano, Appl. Phys. Lett. **87**, 013104 (2005)
25. S. Nakamura, M. Senoh, S. Nagahama, N. Iwasa, T. Yamada, T. Matsushia, H. Kiyoku, Y. Sugimoto, T. Kozaki, H. Umemoto, M. Sano, K. Chocho, Appl. Phys. Lett. **73**, 832 (1998)